4. Seismic Hazard

4.1 Introduction

Seismic hazard, as used in this study, is the expectation of earthquake effects. It is usually defined in terms of ground shaking parameters (e.g., peak ground acceleration, Modified Mercalli Intensity, peak ground velocity) but, broadly speaking, can include or be defined in terms of fault rupture, ground failure, or other phenomena resulting from an earthquake. Seismic hazard is a function of the size, or magnitude of an earthquake, distance from the earthquake, local soils, and other factors, and is independent of the buildings or other items of value that could be damaged. Estimation of seismic hazard can be performed on a deterministic (e.g., Evernden et al., 1981) or probabilistic (Cornell, 1968; McGuire, 1974; Scawthorn et al., 1978; Algermissen and Perkins, 1976; Algermissen, and Perkins, 1982) basis, depending on the needs of the users. In either case, the methodology follows a process beginning with the definition of seismic sources, based in part on historic seismicity.

The historical record of earthquakes in the United States is relatively short--the only data available for earthquakes prior to about 1900 are historical accounts of earthquake effects (Coffman et al., 1982), which have been used to estimate the distribution of intensities, and the locations and magnitudes of earthquakes. The record of large earthquakes in the 19th century is reasonably well documented for the eastern United States but not for other parts of the country. The large 1857 Ft. Tejon event, for example, is not well documented, when compared with the documentation for the 1886 Charleston, South Carolina event (Dutton, 1887). Instrumental data from stations in the United States were not available until after 1887 (Poppe, 1979) when the first seismograph stations in the country were established at Berkeley and Mt. Hamilton (Lick Observatory).

4.2 Magnitude and Intensity

The earthquake magnitude scale is a well-known but typically misunderstood means of describing the energy released during an earthquake. The best-known scale is that developed by C. F. Richter (Richter, 1958); and relationships between the Richter scale and other scales have been established. Magnitude scales are intended to be objective, instrumentally determined measures of the size of an earthquake, and a number of magnitude scales have been developed since Richter's (Aki and Richards, 1980). The most recent widely used scale is moment magnitude, M_W (Hanks and Kanimori, 1979). An increment in magnitude of one unit (i.e., from magnitude 5.0 to 6.0) represents an increase of approximately 32 times the amount of energy released. Unless otherwise noted, earthquake magnitude as used in this study refers to surface wave magnitude, M_S.

While *magnitude* describes the size of an earthquake, *intensity* describes its effects at a particular location or site. Intensity at a site is governed by the magnitude of an earthquake, the distance from the site to the earthquake epicenter or rupture surface, and local geologic conditions. A small or moderate earthquake may generate strong ground shaking, but the areal extent of this shaking will be substantially less than that generated by a major earthquake. The 1931 Modified Mercalli Intensity (MMI) Scale (Wood and Neumann, 1931, Table 4-1) is a commonly used measure of intensity. The scale consists of 12 categories of ground motion intensity, from I (not felt, except by a few people) to XII (total damage). Structural damage generally is initiated at about MMI VI for poor structures, and about MMI VIII for good structures. MMI XI and XII are extremely rare. The MMI scale is subjective; it is dependent on personal interpretations and is affected, to some extent, by the quality of construction in the affected area. Even though it has these limitations, it is still useful as a general description of damage, especially at the regional level, and for this reason will be used in this study, as the descriptor of seismic hazard.

4.3 Earthquake Hazards

Physical damage to structures and lifelines during and after an earthquake can be produced by ground shaking, fault rupture, landslides,

Table 4-1 Modified Mercalli Intensity Scale

I. Not felt. Marginal and long-period effects of large earthquakes.

II. Felt by persons at rest, on upper floors, or favorably placed.

III. Felt indoors. Hanging objects swing. Vibration like passing of light trucks. Duration estimated. May not be recognized as an earthquake.

IV. Hanging objects swing. Vibration like passing of heavy trucks; or sensation of a jolt like a ball striking the walls. Standing motor cars rock. Windows, dishes, doors rattle. Glasses clink. Crockery clashes. In the upper range of IV wooden walls and frames creak.

V. Felt outdoors; direction estimated. Sleepers wakened. Liquids disturbed, some spilled. Small unstable objects displaced or upset. Doors swing, close, open. Shutters, pictures move. Pendulum clocks stop, start, change rate.

VI. Felt by all. Many frightened and run outdoors. Persons walk unsteadily. Windows, dishes, glassware broken, knickknacks, books, etc., off shelves. Pictures off walls. Furniture moved or overturned. Weak plaster and masonry D cracked. Small bells ring (church, school). Trees, bushes shaken (visible, or heard to rustle).

VII. Difficult to stand. Noticed by drivers of motor cars. Hanging objects quiver. Furniture broken. Damage to masonry D, including cracks. Weak chimneys broken at roof line. Fall of plaster, loose bricks, stones, tiles, cornices (also unbraced parapets and architectural ornaments). Some cracks in masonry C. Waves on ponds; water turbid with mud. Small slides and caving in along sand or gravel banks. Large bells ring. Concrete irrigation ditches damaged.

VIII. Steering of motor cars affected. Damage to masonry C; partial collapse. Some damage to masonry B; none to masonry A. Fall of stucco and some masonry walls. Twisting, fall of chimneys, factory stacks, monuments, towers, elevated tanks. Frame houses moved on foundations if not bolted down; loose panel walls thrown out. Decayed piling broken off. Branches broken from trees. Changes in flow or temperature of springs and wells. Cracks in wet ground and on steep slopes.

IX. General panic. Masonry D destroyed; masonry B seriously damaged. (General damage to foundations.) Frame structures, if not bolted, shifted off foundations. Frames racked. Serious damage to reservoirs. Underground pipes broken. Conspicuous cracks in ground. In alluviated areas sand and mud ejected, earthquake fountains, sand craters.

X. Most masonry and frame structures destroyed with their foundations. Some well-built wooden structures and bridges destroyed. Serious damage to dams, dikes, embankments. Large landslides. Water thrown on banks to canals, rivers, lakes, etc. Sand and mud shifted horizontally on beaches and flat land. Rails bent slightly.

XI. Rails bent greatly. Underground pipelines completely out of service.

XII. Damage nearly total. Large rock masses displaced. Lines of sight and level distorted. Objects thrown into the air.

Source: Richter, C.F., 1957, *Elementary Seismology*, W. H. Freeman Co., San Francisco, Calif.

Note: To avoid ambiguity, the quality of masonry, brick, or other material is specified by the following lettering system. (This has no connection with the conventional classes A, B, and C construction.)

Masonry A. Good workmanship, mortar, and design; reinforced, especially laterally, and bound together by using steel, concrete, etc.; designed to resist lateral forces.

Masonry B. Good workmanship and mortar; reinforced, but not designed to resist lateral forces.

Masonry C. Ordinary workmanship and mortar; no extreme weaknesses, like failing to tie in at corners, but neither reinforced nor designed to resist horizontal forces.

Masonry D. Weak materials, such as adobe; poor mortar; low standards of workmanship; weak horizontally.

liquefaction, and earthquake-induced fire. Ground shaking is the primary and best-known hazard associated with earthquakes. It produces scattered but widespread damage. Ground shaking includes both horizontal and vertical motions, can last up to several minutes during major earthquakes, and can be destructive at distances of even hundreds of kilometers, depending on soil conditions. It is estimated that such shaking causes over 90% of earthquake-related damage to buildings.

Ground or fault rupture produces local concentration of structural damage. A *fault* is a fracture in the crust of the earth along which blocks have moved or been displaced in relation to each other. This displacement can be in either a horizontal, a vertical, or an oblique direction. Near fault lines, fault displacements produce forces so great that the best method of limiting damage to structures is to avoid building in areas close to ground traces of active faults.

Secondary seismic hazards are those related to soil instabilities. *Liquefaction* is the sudden loss of shear strength that can occur when saturated, soils that lack cohesion (sands and silts) are strongly and repetitively vibrated. Liquefaction typically occurs in loose sand deposits where there is subsurface groundwater above a depth of about 20 feet. Shallow groundwater and loose soil are usually localized conditions, resulting either from natural or human-made causes. As a result, site-specific data generally are necessary to accurately determine if liquefaction may occur at a location. It usually severely damages civil engineering works and low-rise buildings. Mid- and high-rise buildings in these soils will tend to have pile foundations, which mitigate the structural effects of liquefaction, or reduce liquefaction potential, but may not completely eliminate the threat.

Settlement or compaction of loose soils and poorly consolidated alluvium can occur as a result of strong seismic shaking, causing uniform or differential settlement of building foundations. Buildings supported on deep (pile) foundations are more resistant to such settlements. Substantial compaction can occur in broad flat valley areas recently depleted of groundwater.

Landslide is the downslope movement of masses of earth under the force of gravity. Earthquakes can trigger landslides in areas that are already landslide prone. Slope gradient is often a clue to stability. Landslides are most common on slopes of more than 15^{0} and can generally be anticipated along the edges of mesas and on slopes adjacent to drainage courses.

4.4 Seismicity

Seismicity is the space-time occurrence of earthquakes. The historical seismicity of the United States is shown in Figure 4-1, which depicts the spatial distribution of earthquakes with maximum MMIs of V or greater, known to have occurred through 1976. For the purpose of characterizing seismicity in the conterminous United States, several regions may be identified (Algermissen, 1983), as shown in Figure 4-2:

1. Northeastern Region, which includes New England, New York, and part of eastern Canada;

2. Southeastern Region, including the central Appalachian seismic region activity and the area near Charleston, South Carolina;

3. Central Region, which consists of the area between the regions just described and the Rocky Mountains;

4. Western Mountain Region, which includes all remaining states except those on the Pacific coast;

5. Northwestern Region, including Washington and Oregon; and

6. California and Western Nevada.

We discuss each of these regions briefly largely using information from Algermissen (1983) and Coffman et al. (1982). These references can provide a more detailed discussion.

Northeastern Region. The Northeastern Region contains zones of relatively high seismic activity--earthquakes of at least magnitude 7.0 have occurred in New England and the St. Lawrence River Valley in Canada (Algermissen, 1983). The historic seismicity of this region is shown in Figure 4-3.

One of the largest earthquakes to have affected this area was the November 18, 1755,

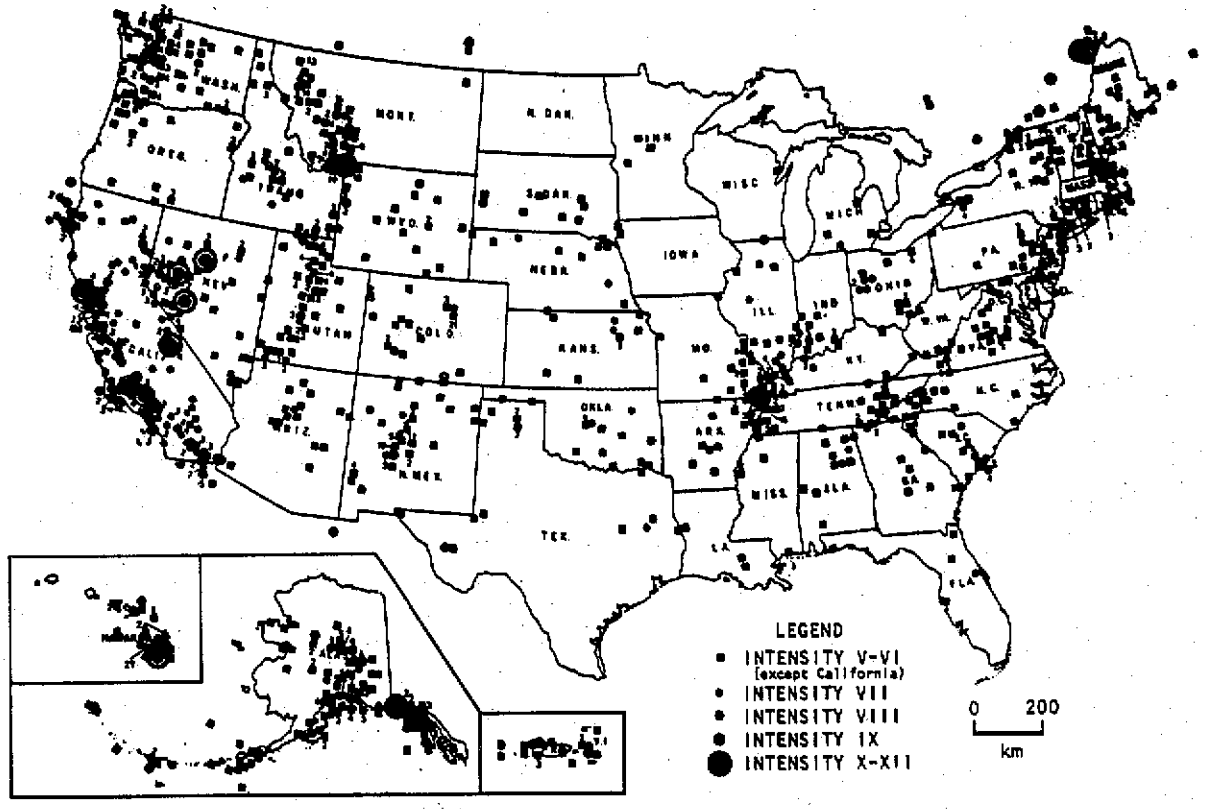

Figure 4-1 *Earthquakes with maximum Modified Mercalli Intensities of V or above in the United States and Puerto Rico through 1989 (Algermissen, 1983, with some modifications).*

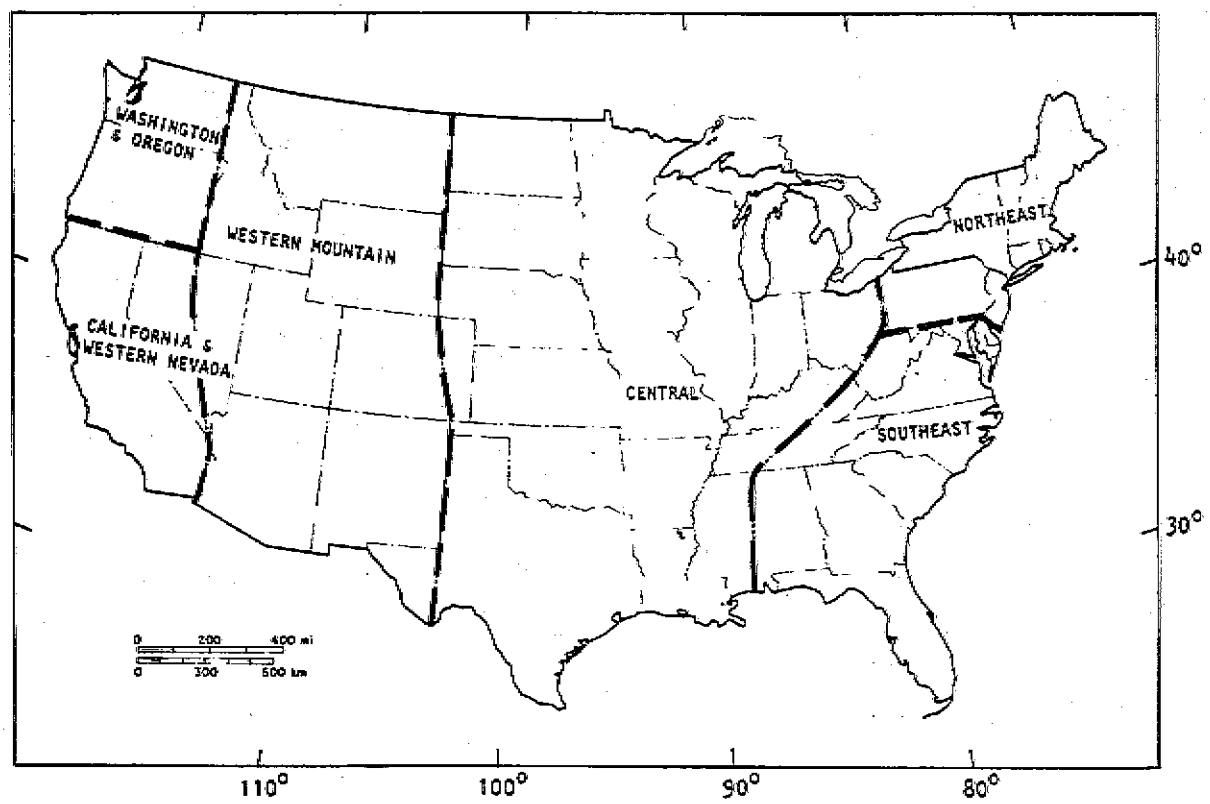

Figure 4-2 *Regional scheme used for the discussion of the seismicity of the conterminous United States.*

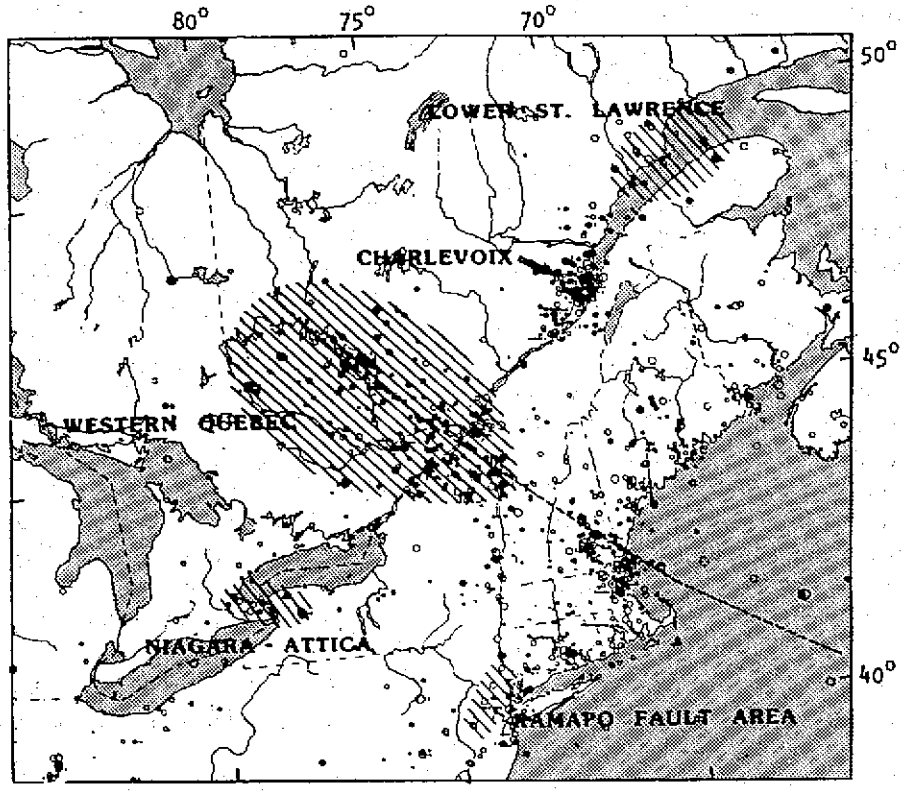

Figure 4-3 *The seismicity of the northeastern region of the United States and Eastern Canada for the period 1534-1959 (from Algermissen, 1983). The solid circles are principally instrumentally determined epicenters, while the open circles represent earthquakes located in using intensity data. The hachured and named areas represent concentrations of seismicity grouped together only for the purpose of discussion in the text. The dashed line represents the strike of the New England (Kelvin) sea mount chain offshore. Onshore, the line has been extended to show the northwest-southwest alignment of seismicity known as Boston-Ottawa trend.*

earthquake east of Cape Ann, with an epicenter located at about 42.5 N and 70.0 W, with magnitude 6.0 (magnitude and epicenter location estimated on the basis of seismic intensity data). The shock was felt from Chesapeake Bay to Annapolis River, Nova Scotia; and from Lake George, New York, to a point at sea 200 miles east of Cape Ann, an area of about 300,000 square miles.

Southeastern Region. The seismicity of this region is shown in Figure 4-4. With the exception of the Charleston, South Carolina, earthquake, this region has a moderate level of earthquake activity. The largest and by far the most destructive earthquakes in this region occurred on August 31, 1886, with their epicenter about 15 miles northwest of Charleston, South Carolina (32.9 N, 80.0 W). The first shock was at 21:51, the second about 8 minutes later. An area with a radius of 800 miles was affected; the strongly shaken portion extended to 100 miles.

The bending of rails and lateral displacement of tracks due to ground displacements were very evident in the epicentral region, though not at Charleston. There were severe bends of the track in places and sudden and sharp depressions of the roadbed. At one place, there was a sharp S-curve. At a number of locations, the effect on culverts and other structures demonstrated strong vertical force in action at the time of the earthquake. Figure 4-5 shows the effects in the epicentral area, and Figure 4-6 shows the isoseismal map for the event (Bollinger, 1977).

Central Region. Compared to the interior of other continents, the central region of North America, especially the Upper Mississippi embayment, is one of relatively frequent small-to-moderate size earthquakes and infrequent large events. In fact, three of the largest earthquakes in North American history occurred there (Hopper, 1985). These latter events occurred in 1811-1812, near the present town of New Madrid, Missouri. They were powerful enough to alter the course of the Mississippi River. Although masonry and stone structures were damaged to distances of 250 kilometers, and chimneys destroyed to distances of 400 kilometers, the sparse settlement of the area prevented grave damage. The extent and severity of ground failure and topographic effects from these shocks have not been equaled by any other earthquake in the conterminous United States.

The seismicity of this region is shown in Figure 4-7. Earthquakes of small magnitude (less than 5.0) are scattered throughout the region, and the major seismicity is associated with the rift structure identified in the New Madrid area. Since the 1811-1812 sequence, nine events of estimated magnitude greater than 5.0 have occurred through 1980, only one of which is estimated to have been greater than magnitude 6.0 (m_b 6.2, in 1895) (Algermissen, 1983).

The New Madrid Seismic Zone lies within a 40-mile-wide, 120-mile-long portion of the northern Mississippi embayment--a south-plunging trough of sedimentary rocks. The boundaries of this zone are at present somewhat uncertain. The zone may extend farther to the south than presently recognized. The epicenter pattern in the New Madrid area shows well-defined lineations: a northeast-striking zone that extends about 60 miles from near Marked Tree, Arkansas (approximately 40 miles northwest of Memphis), to near Caruthersville, Missouri; a north-northwest-striking zone from southeast of Ridgely, Tennessee, to west of New Madrid; and another northeast-striking zone extending from west of New Madrid to near Charleston, Missouri. The first zone is less active, but earthquakes along it have relatively higher magnitudes. The third zone includes frequent events of small magnitude. Note that no identifiable surface faults or offset landforms or drainage features have been identified.

Because seismic attenuation through frictional damping, or dissipation of earthquake energy with distance, is less in the eastern and central United States than in the west, earthquakes in this area have the potential or producing strong ground shaking over comparatively wide areas. The isoseismal map of the December 16, 1811, New Madrid earthquake (Nuttli, 1981) is shown in Figure 4-8. Algermissen and Hopper (1985) have developed maps of hypothetical intensities for the region, based on enveloping effects that would result from an earthquake occurring "anywhere from the northern to southern end of the seismic zone."

Western Mountain Region. Important earthquake activity in this region has occurred in

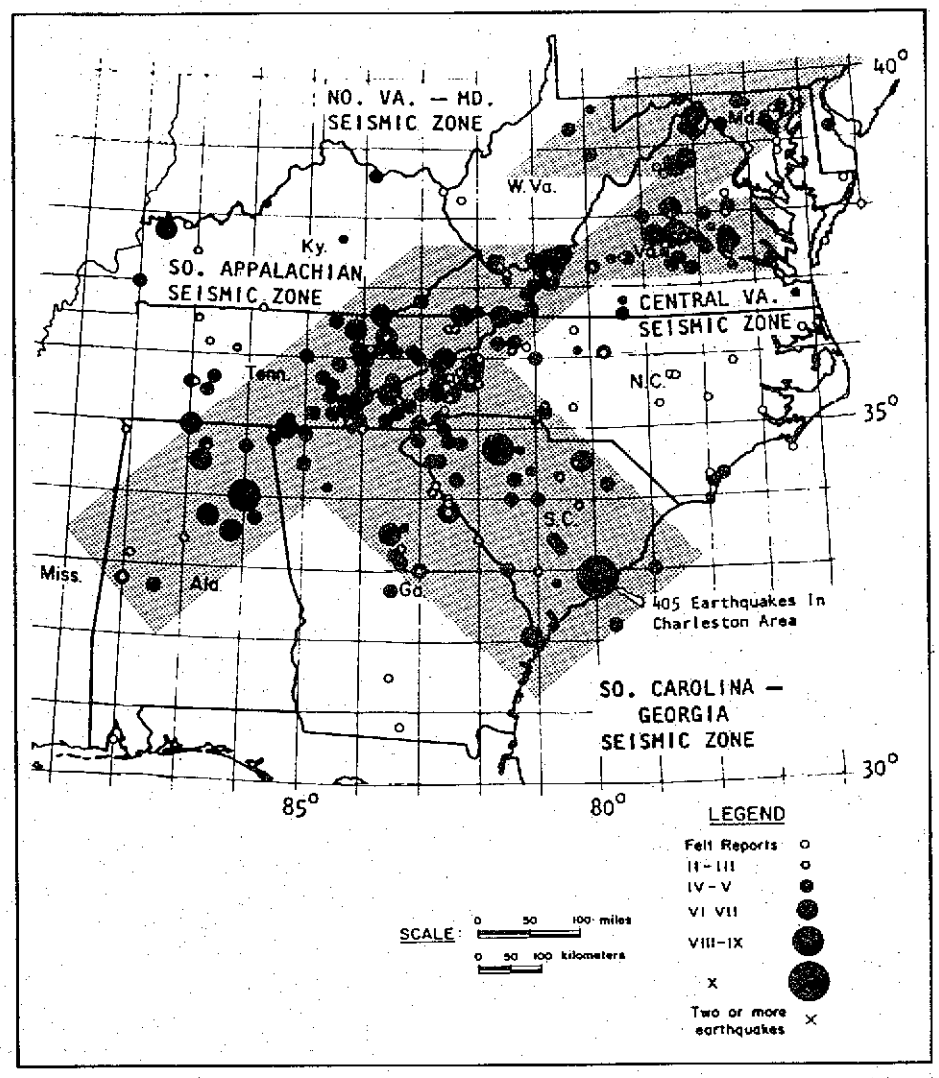

Figure 4-4 *Seismicity of the Southeastern region, 1754-1970 (from Bollinger, 1977).*

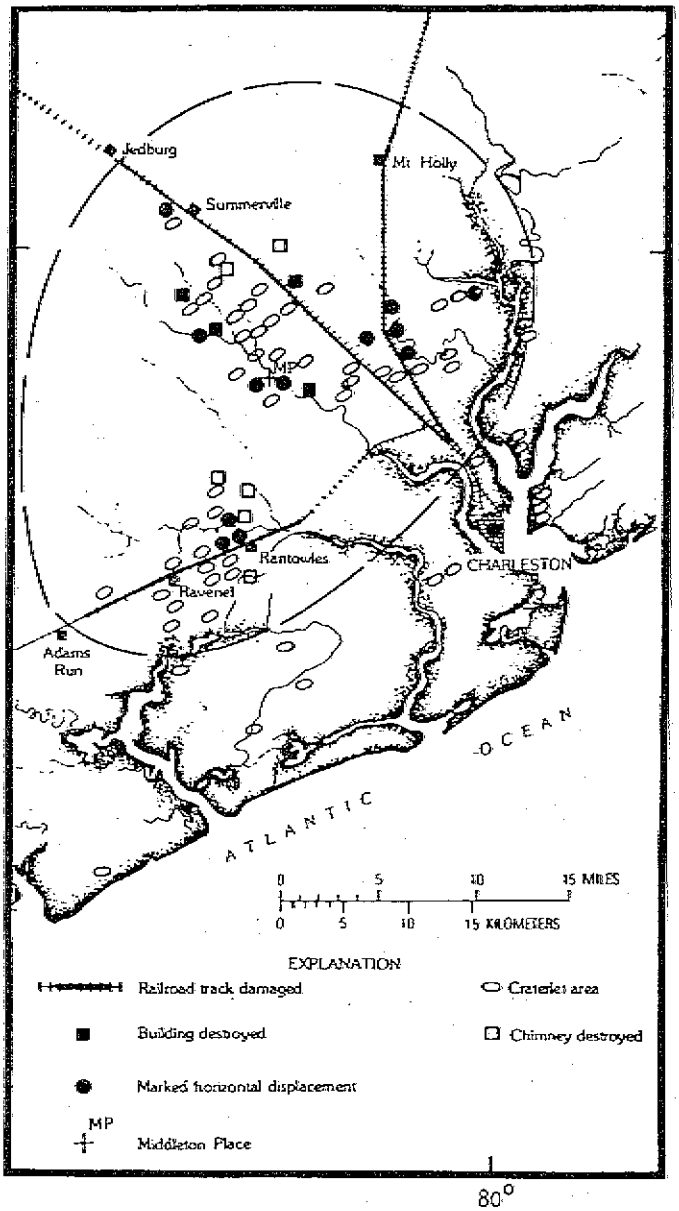

Figure 4-5 *Effects in the epicentral area of the 1886 Charleston, South Carolina, Earthquake (from Algermissen, 1983).*

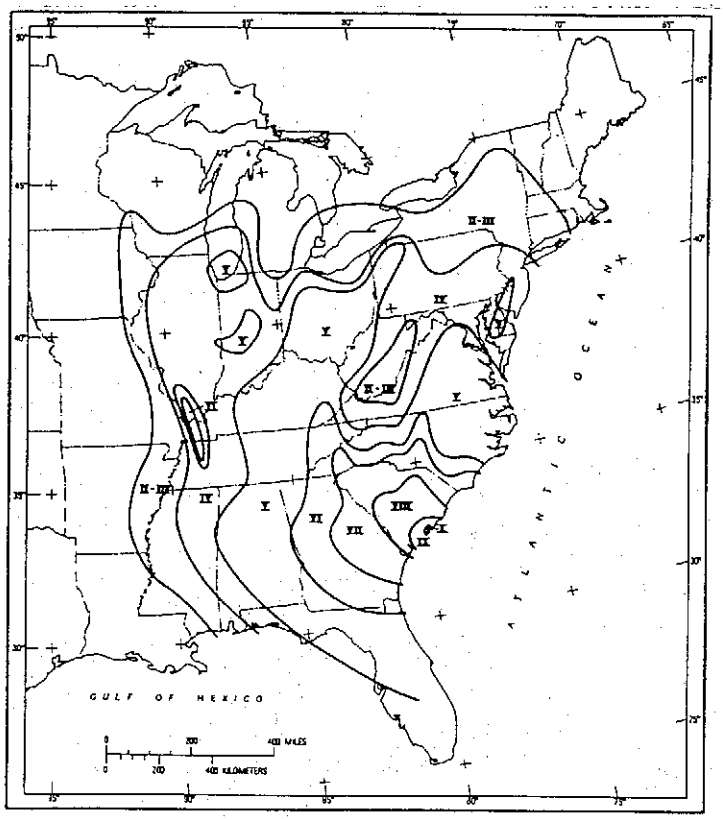

a) Broad map, based on detailed map (below)

b) Detailed map of seismic intensity.

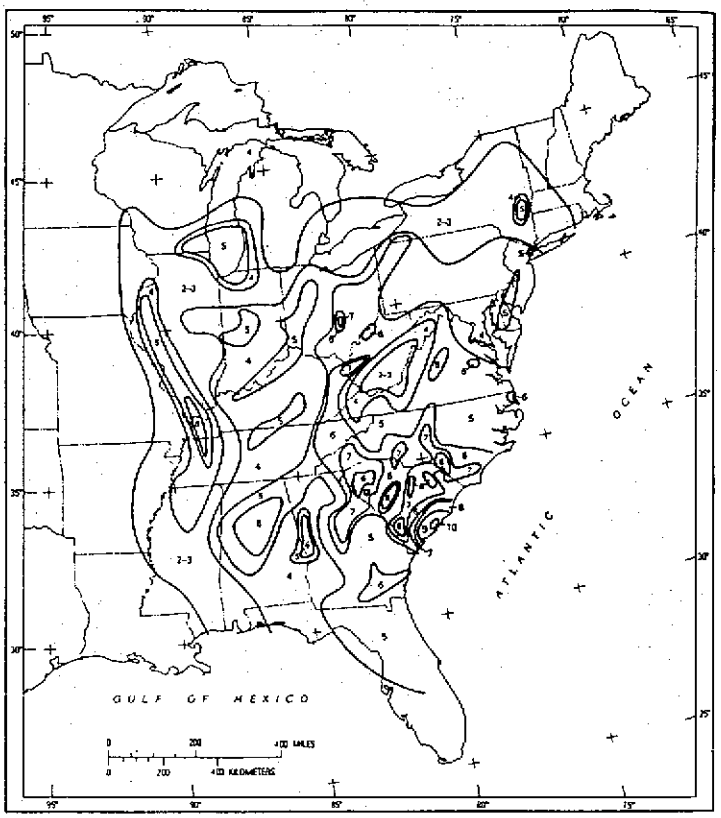

Figure 4-6 *Isoseismal map of the 1886 Charleston, South Carolina, Earthquake (from Bollinger, 1977).*

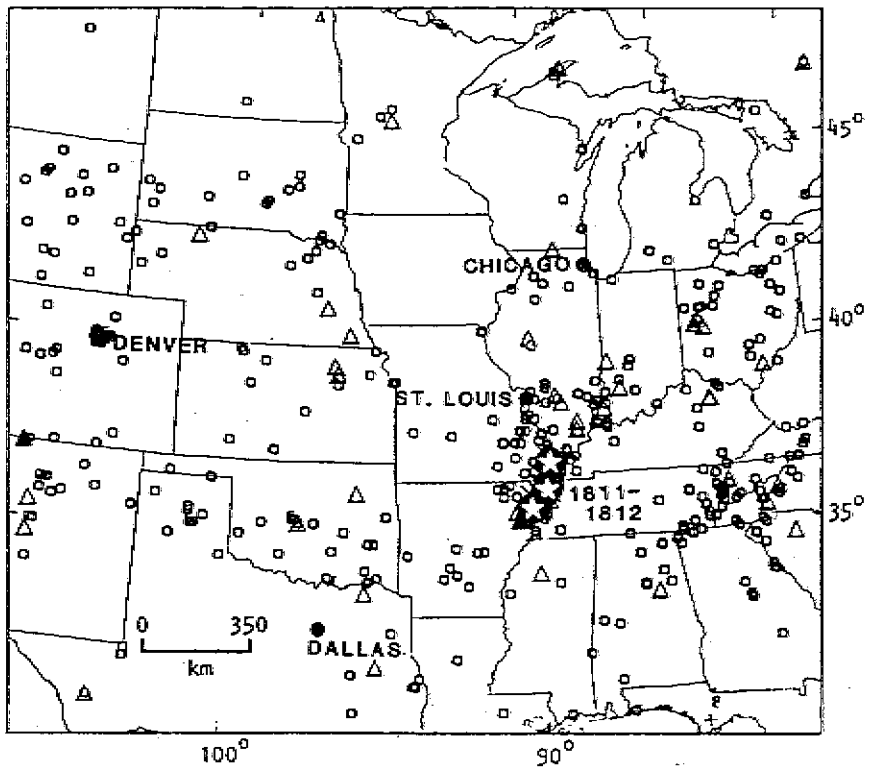

Figure 4-7 *Seismicity of the Central Region, 1811-1976. The data are taken principally from Algermissen (1983) with minor changes and additions. The stars represent earthquakes with maximum MMIs of IX or greater; triangles represent earthquakes with maximum intensities of VII-VIII; squares represent earthquakes with maximum intensities of V-VI.*

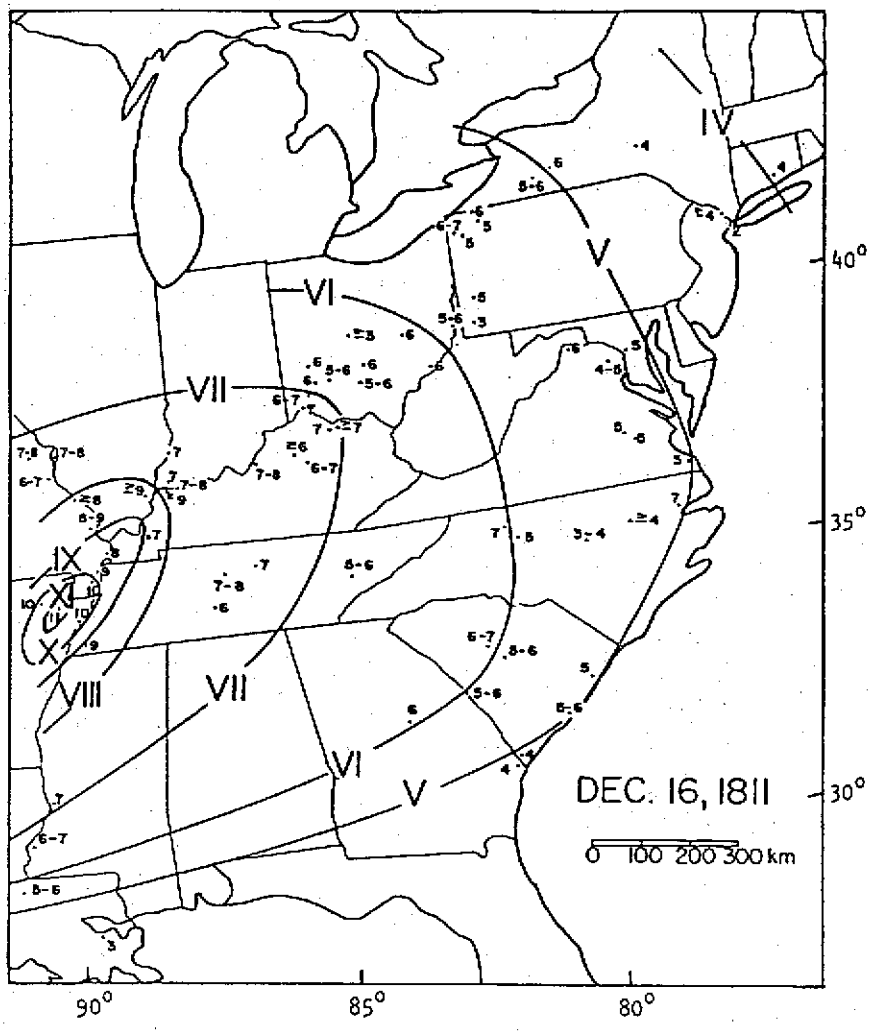

Figure 4-8 *Isoseismal map of the December 16, 1811, earthquake (from Nuttli, 1979). The Arabic numbers give the Modified Mercalli intensities at each data point.*

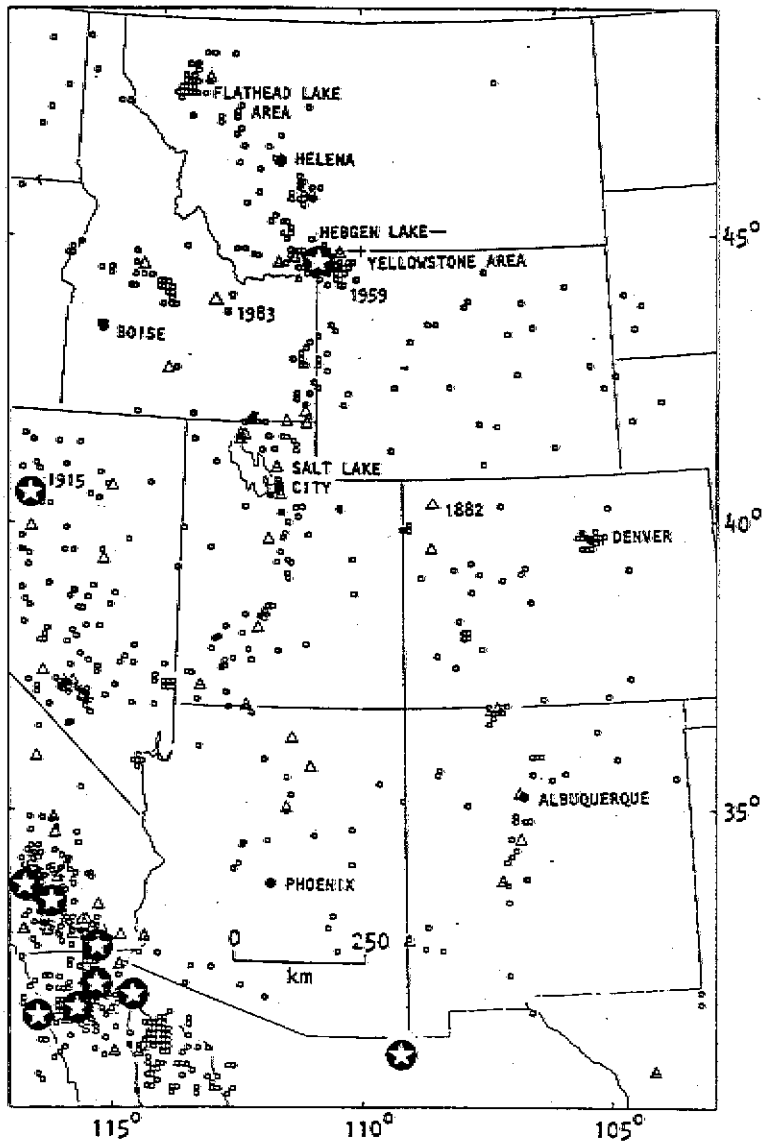

Figure 4-9 *Seismicity of the Western Mountain Region (Algermissen, 1983). Stars represent earthquakes with maximum intensities of IX or greater; triangles represent earthquakes with maximum intensities of VII-VIII; and squares represent earthquakes with maximum intensities of V-VI.*

the Yellowstone Park-Hebgen Lake area, in western Montana, in the vicinity of the Utah-Idaho border, and sporadically along the Wasatch Front, as shown in Figure 4-9. Major earthquakes occurred in Helena, Montana, in 1925 (M_s 6.7), at Hebgen Lake, Montana, in 1959 (M_s 7.1) and at Borah Peak, Idaho, in 1983 (M_s 7.3).

Probably the most serious risk in the Western Mountain Region, however, exists along the Wasatch Front region of north-central Utah. This area is dominated by the Wasatch Fault, a 220-mile-long, north-south-trending zone extending from Gunnison, Utah, in the south, to Malad City, Idaho, in the north, and directly threatening the Salt Lake City area. In this zone, young mountain blocks have been uplifted to form the prominent west-facing scarp (the Wasatch Front), which forms the eastern boundary of the Salt Lake and Utah valleys. Included in this zone is the active East Cache Fault System located on the eastern side of Cache Valley. Another related fault system of interest is the Hansel Valley Fault Zone, located north of the Great Salt Lake near the border with Idaho. It has been the most active fault in the state for larger-size events (Arabasz and Smith, 1979).

Historic records of earthquake activity in Utah date back to 1853, shortly after the region was settled permanently. Since that time, over 1,000 felt events have occurred on a regular basis. The earliest event recorded that has been estimated to have a magnitude of 6.0 or greater was the Bear Lake Valley Earthquake in 1884 (estimated magnitude 6.1). The 1909 event in Hansel Valley was assigned a maximum intensity of VIII and a magnitude of 6.0, and resulted in waves being sent over the railway causeway at the north end of the Great Salt Lake and windows being broken as far away as Salt Lake City. The largest earthquake to date in Utah, the 1934 Hansel Valley event (M_s 6.6) severely damaged brick buildings in Kosmo, produced 2-foot scarps in the ground surface, greatly altered groundwater flow patterns, and caused nonstructural damage to buildings in Salt Lake City. It occurred in a sparsely populated area, otherwise great damage could have resulted.

Historic earthquake damage to the Utah Valley area has thus far been due to local earthquakes with magnitudes of approximately 5.0 or less, with maximum intensities of about MMI VI or less. Damage has been mostly limited to cracked walls and chimneys, and broken windows. Since 1960, there has been very little notable earthquake activity in the Utah Valley. However, research has shown that many large seismic events (magnitudes 6.5 to 7.5) have taken place along the Wasatch Front during the past 10,000 years (Swan et al, 1980).

Northwestern Region. The seismicity of Washington and Oregon is shown in Figure 4-10. Most of the earthquake activity has occurred in the vicinity of Puget Sound. Although a few geologically recent faults thought to be potentially active have been located in western and central Washington, no historic seismic activity has been associated with them. Instead, most recorded seismic activity in Washington has been attributed to the subduction of the offshore Juan de Fuca crustal plate beneath the North American continental plate.

Subduction zones occur at locations where, under the influence of tectonic plate movement, one piece of the earth's crust is forced beneath another. Subduction zones have been associated with very large earthquakes including the 1985 Mexico City (M_s 8.1) and 1964 Alaska (M_s 8.3) events. Subduction zones are frequently associated with volcanic activity as well as earthquakes. The presence of the volcanically active Cascade range supports the evidence for an active Juan de Fuca subduction zone. Further supporting evidence includes the mountains on the Olympic peninsula, which appear to have been formed by debris scraped off the Juan de Fuca plate by the overriding North American plate.

Available geologic information indicates that great earthquakes, with magnitudes in excess of 8.0, have occurred on the Juan de Fuca subduction zone at least eight times in the last 5,000 years. The last such event is thought to have occurred about 300 years ago. Evidence for such an earthquake includes geologically recent submerged marsh lands and fossil forests along the Washington coastline. It is believed that portions of the Washington coast subsided by as much as 3 feet in that event.

In addition to the great earthquakes described above, extensive but more moderate seismicity

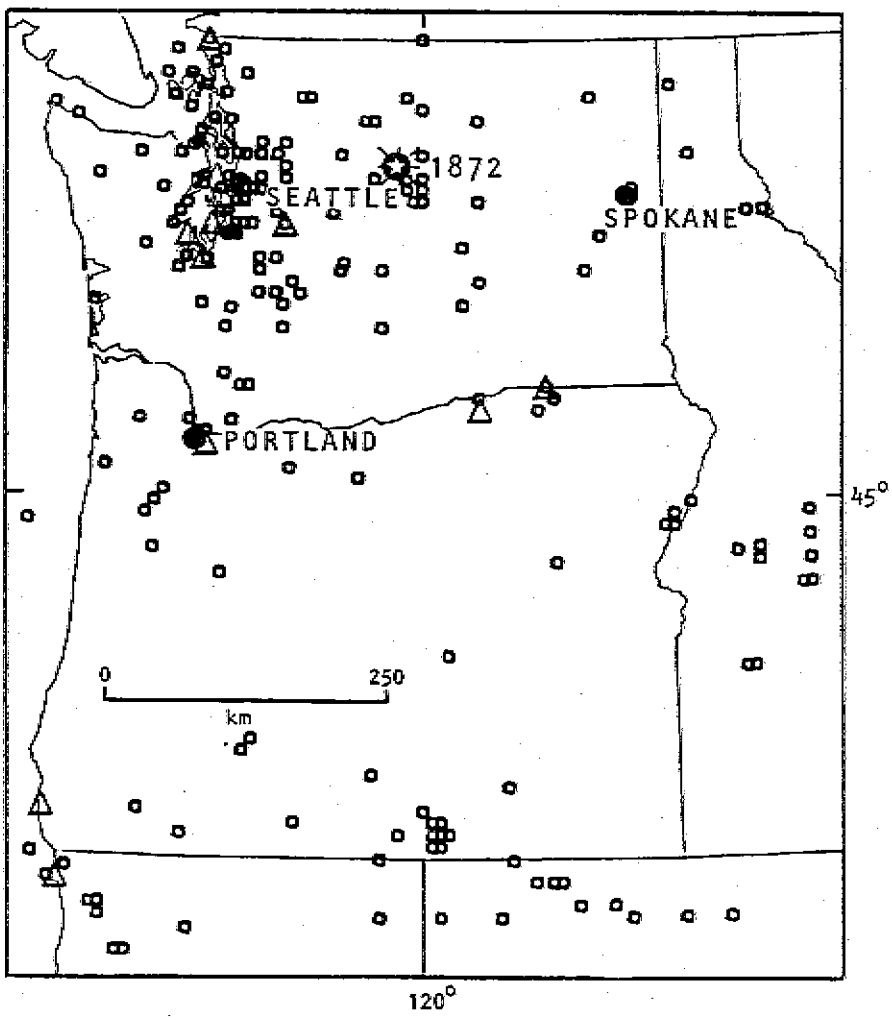

Figure 4-10 *Seismicity of Oregon and Washington, 1859-1975. The star represents an earthquake with maximum Modified Mercalli intensity of IX; triangles represent earthquakes with maximum intensities of VII-VIII; and small squares represent earthquakes with maximum intensities of V-VI (Algermissen, 1983).*

has been associated with the same subduction zone, deep beneath the Puget Sound trough between Seattle and Olympia. In this area, termed the Puget Trough Intercrustal Zone, the friction between the underlying Juan de Fuca plate and overriding North American plate has resulted in many mid-size events with occasional strong damaging shocks. Typically these events occur at depths from 20 to 30 miles below the surface and are therefore less damaging than events of similar size in California, which occur at shallower depths. Two of the largest recorded earthquakes in the Pacific Northwest have occurred in this zone. A M_S 7.1 event in 1949, located near Olympia, caused extensive damage in Seattle, Tacoma, and Olympia. A 1965 (M_S 6.5) event, centered near the Seattle-Tacoma airport, caused MMI VII and VIII damage in both Seattle and Tacoma. A mean return period of approximately 30 years has been calculated for events of this size. Great earthquakes of magnitude 7.5 or larger are believed credible.

An earthquake in the northern Cascades in 1872 had an estimated magnitude of 7.3 and a maximum intensity of MMI IX. Earthquake intensities of MMI VII were experienced on the Olympic peninsula in 1891 and again in 1904. Two moderate earthquakes in 1932 and 1945 shook the central Cascades with maximum MMI VII.

The Vancouver-Victoria area, located in the northern portion of Puget Sound, has had a relatively large number of smaller earthquakes. However, the maximum magnitudes experienced have been much lower than those in the southern portion of Puget Sound. Only three earthquakes as large as magnitude 5.5 have occurred in the Vancouver-Victoria area. The corresponding maximum intensities were on the order of MMI VII. The estimated maximum magnitude for the Vancouver-Victoria area is about 6.5.

Further north on Vancouver Island, over 200 miles from Seattle, two earthquakes of magnitudes 7.0 and 7.4 occurred in 1918 and 1946, respectively. These events produced maximum intensities of MMI VIII but did not cause significant damage in Washington.

California and Western Nevada. Earthquakes in California and Western Nevada represent a high percentage of the seismic activity of the conterminous United States. The majority of these shocks occur at relatively shallow focal depths of 10 to 15 miles and along known rupture zones or faults. Figure 4-11 shows the seismicity of this region, while Figure 4-12 shows faults with historic displacements in this region.

While this area is the most seismically active region of the conterminous United States, only three events with magnitudes greater than M_S 8.0 have occurred in historical times. Two of these events occurred on the principal fault in this area, the San Andreas, which extends over 600 miles through California, from near the Salton Sea in Southern California northwest to Cape Mendocino. The most famous of these San Andreas events was the April 18, 1906, San Francisco Earthquake (M_S 8.3), caused by a rupture of approximately 270 miles in length, from San Juan Bautista to off Cape Mendocino. Devastation was extremely widespread, with enormous losses in San Francisco caused by the ensuing conflagration (Lawson et al., 1908). The other of these events, the Ft. Tejon Earthquake, occurred on January 9, 1857, on a segment of the San Andreas Fault between Cholame and south of Cajon Pass. It may be regarded as a Southern California counterpart of the 1906 event. The isoseismal maps for these events are shown in Figure 4-13. In addition to these two great earthquakes, a number of large, potentially damaging earthquakes have occurred on the San Andreas Fault, including events in 1838, 1865, and, most recently, the October 17, 1989, Loma Prieta Earthquake (M_S 7.1). This last event resulted in very significant disruption to almost all lifelines, especially the highway and electric power networks (Khater et al., 1990).

The third of the great historic California earthquakes is the 1872 Owens Valley event, resulting from approximately 150 kilometers of faulting. The area was relatively sparsely populated but still resulted in about 10% fatalities in Lone Pine, because of the predominantly adobe construction.

Another very important fault in Northern California is the Hayward Fault, located on the eastern side of San Francisco Bay and extending approximately 55 miles from San Jose northwesterly to San Pablo (Figure 4-12). The Hayward Fault is one of the major active branches of the San Andreas Fault System, and is particularly significant because it passes

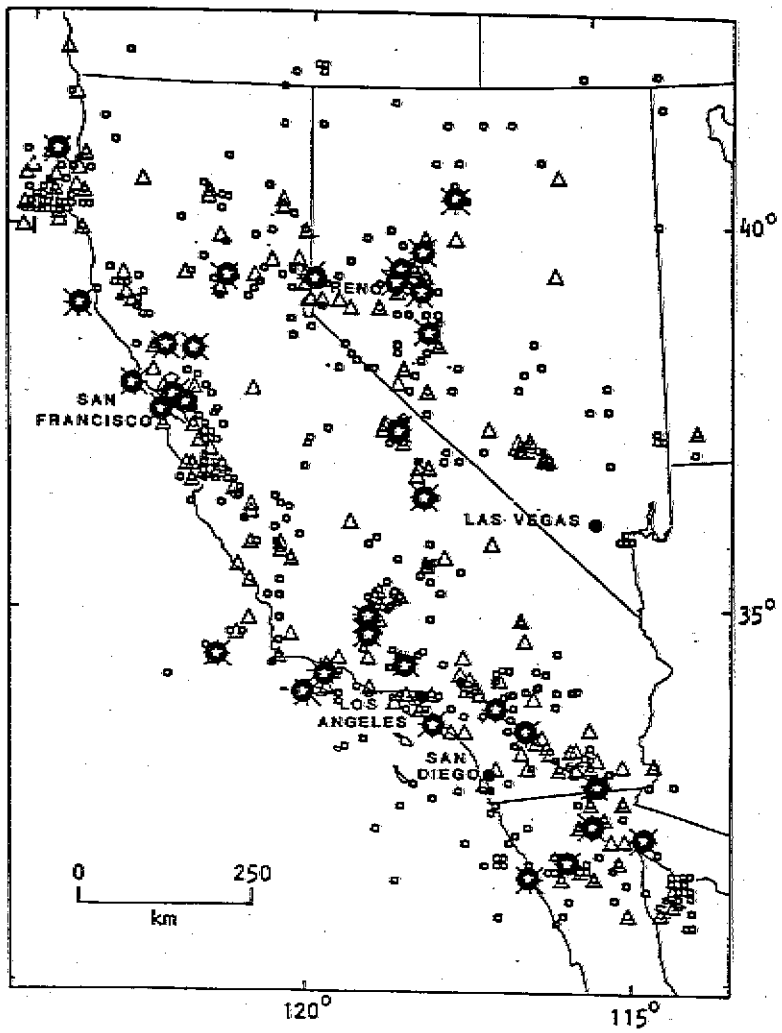

Figure 4-11 *Seismicity of Western Nevada and California, 1811-1976 (Algermissen, 1983). Stars represent earthquakes with Modified Mercalli intensities of IX or greater, triangles represent shocks with maximum intensities of VII-VIII; and small squares represent shocks with maximum intensities of VI.*

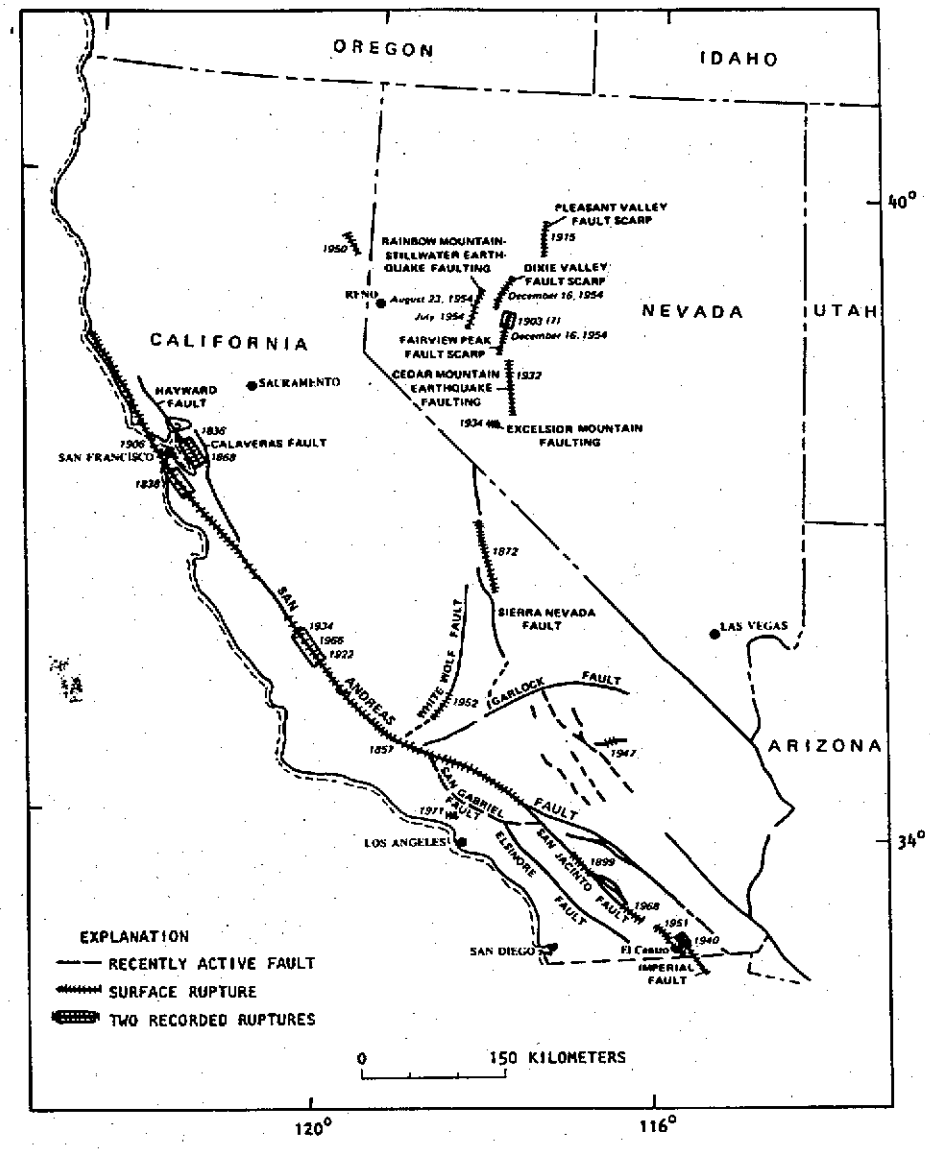

Figure 4-12 *Faults with historic displacements in California and Nevada. The year of occurrence for selected large earthquakes is shown (Algermissen, 1983).*

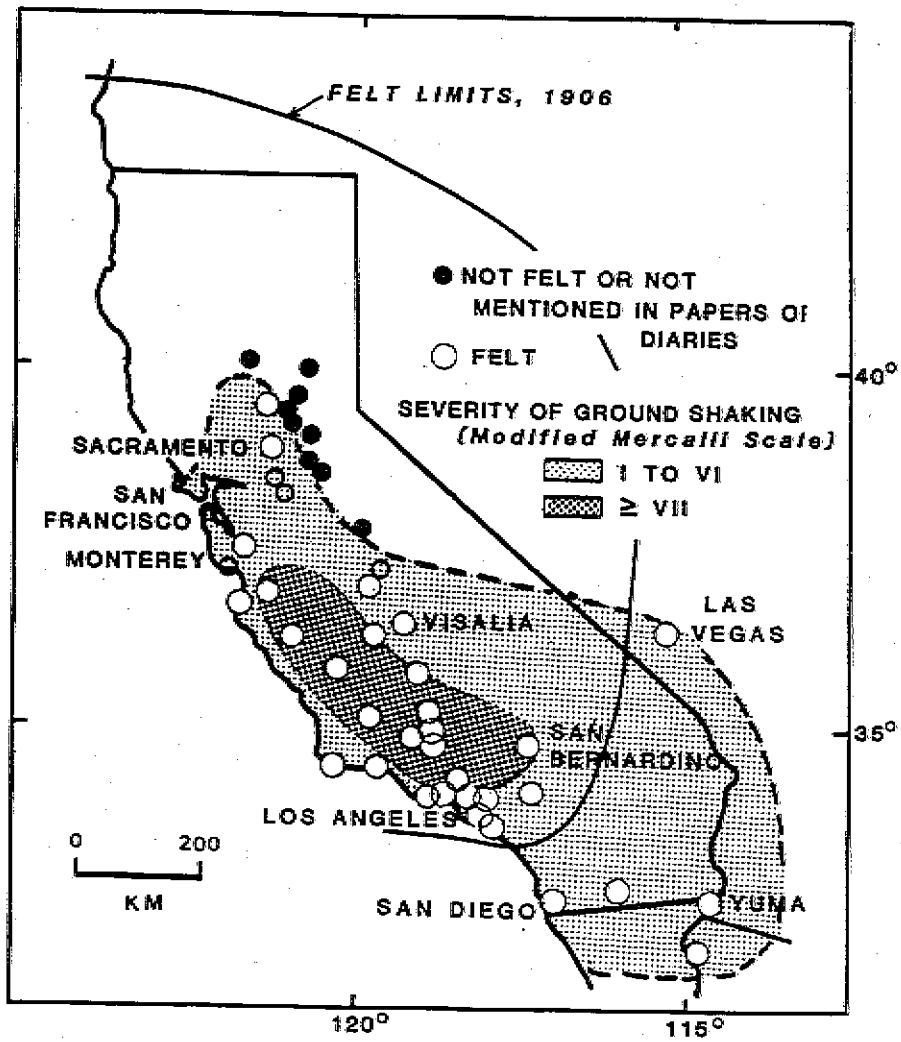

Figure 4-13 *Isoseismal map for the January 9, 1857, earthquake on the San Andreas Fault near Fort Tejon (Algermissen, 1983). Also shown, for comparison, are the felt limits for the 1906 San Francisco Earthquake.*

directly through the heavily populated cities such as Hayward, San Leandro, Oakland, and Berkeley. It was the source of the Hayward Earthquake of 1836 (estimated M_S 6.8), in which fissures opened along the fault from San Pablo to Mission San Jose, and ground shaking caused havoc in the settlements of San Jose and Monterey. In 1868 an earthquake (estimated M_S 6.8) ruptured the fault the fault for 20 miles and severely damaged every building in the village of Hayward. More recent damaging earthquakes occurred in 1915, 1933, and 1937. The Hayward Fault is believed capable of producing earthquakes as large as magnitude 7.5, and is presently judged highly likely to rupture with a magnitude of about 7.0 in the near future [United States Geological Survey (USGS), 1990]; this judgment is based, among other evidence, on the pairing of San Andreas/Hayward events in 1838/1836 and 1865/1868. A large earthquake on this fault is of potentially catastrophic proportions (Steinbrugge et al., 1987).

Similar to the Hayward Fault situation in the San Francisco Bay Area, the Los Angeles region is threatened by a number of additional faults, including the Newport-Inglewood, Santa-Monica Raymond, Elsinore, Norwalk, and other faults and fault zones. Significant events have included the 1933 Long Beach event (M_S 6.3) on the Newport-Inglewood Fault (NBFU, 1933; Binder, 1952), the 1971 San Fernando event (M_S 6.4, San Fernando Fault), and the 1987 Whittier (M_S 5.9) event.

Other significant events in California have included the 1940 El Centro (M_S 7.1), the 1952 Kern County (M_S 7.7), and the 1983 Coalinga (M_S 6.5) events.

4.5 Regional Representative Earthquakes

Based on the foregoing review of conterminous U.S. regional seismicity, each region appears to have significant historic precedent for a damaging earthquake of potentially catastrophic dimensions. For purposes of examining this potential, the earthquakes indicated in Table 4-2 are representative events for the investigation of lifeline loss estimation and disruption.

Evernden et al. (1981) estimates that these events represent almost the maximum earthquake expected in each area. Review of Algermissen et al. (1982) indicates general agreement.

Table 4-2 Representative Earthquakes for Lifeline Loss Estimation

Region	*Event*
Northeastern	Cape Ann, 1755
Southeastern	Charleston, 1886
Central	New Madrid, 1811-1812
Western Mountain	Wasatch Front, no date
Northwestern	Puget Sound, 1949
Southern California	Fort Tejon, 1857
Northern California	Hayward, 1868

4.6 Estimation of Seismic Intensities and Choice of Scenario Earthquakes for this Project

Choice of a Model. In order to estimate the seismic hazard (i.e., deterministic intensity) of the scenario events over the affected area associated with each event, a model of earthquake magnitude, attenuation, and local site effects is required. For the conterminous United States, two general models were considered: Evernden and Thomson (1985), and Algermissen et al. (1990).

Both models are applicable for the entire conterminous United States, and each offers many advantages but addresses two fundamentally different users. The Algermissen model is oriented toward probabilistic mapping of seismic hazard, while the Evernden model is oriented toward exploration of the effects of deterministic events. Both models were considered for use in this investigation. Selection of one over the other was difficult, but the Evernden model offered the following advantages for this study: (i) verification via comparison with historical events, (ii) incorporation of local soil effects and ready availability of a nationwide geologic database, and (iii) ready availability of closed-form attenuation relations. While determination of seismic intensities is fundamental to the results of this investigation, the choice of one of these models over the other was not felt to be crucial to this study, because (i) the primary purpose of

this study is not the investigation of seismic hazards in the conterminous United States, or comparison of these two models, but rather the performance of selected lifelines; and (ii) both models probably provide similar results in the mean (it should be noted, however, that the two models have not been systematically compared, to the author's knowledge).

Use of the Evernden Model. Attenuation of ground motion away from the epicenter has been estimated by employing Evernden's model (Evernden et al., 1981). The model contains several parameters whose evaluations are based on empirical data. Only three factors in the model are regionally dependent: the local attenuation factor, the length of rupture, and a parameter related to depth of earthquake focus. The local attenuation factor changes significantly across different regions. Its value is about 1.75 in coastal California, 1.5 in eastern California and the Mountain States, 1.25 in the area of the Gulf and Atlantic Coastal plains including the Mississippi Embayment, and 1.0 in the rest of the eastern United States. Rupture length and energy released are related by an empirical relation, which leads to the observation that all major earthquakes of the Eastern United States have fault lengths of 10-to-40 kilometers maximum. With the local attenuation factor and rupture length established, peak intensity at the epicenter serves to establish the depth of focus.

The geological map of the United States published in the *National Atlas of the United States of America* (Gerlich, no date) was used for the complementary geologic base, digitized on a 25- by 25-kilometer grid.

As noted by Evernden et al. (1981), digitization at this resolution generally results in saturated poor ground not constituting the dominant ground condition in any particular grid element. Therefore, the resulting intensities should generally be interpreted as those on bedrock, per Evernden. This study generally concurs with this point, noting however that even the 25- by 25-kilometer digitization captures poor ground conditions in certain important locations, especially in the Mississippi Valley and along the eastern seaboard. As a generalization, intensities estimated by the Evernden model can be considered to provide lower bounds on site intensities.

Table 4-3 Geologic and Ground Condition Units, Conterminous United States (per Evernden et al., 1981)

Units of Geologic Map	*Ground Condition Unit*	*Relative Intensity*
Sedimentary rocks		
Quaternary	A	0.00
Upper Tertiary	B	-1.00
Lower Tertiary	C	-1.50
Cretaceous	D	-2.00
Jurassic and Triassic	E	-2.25
Upper Paleozoic	F	-2.50
Middle Paleozoic	G	-2.75
Lower Paleozoic	H	-2.75
Younger Precambrian	I	-2.75
Older Precambrian	J	-3.00
Volcanic rocks		
Quaternary and Tertiary volcanic rocks	K	-3.00
Intrusive rocks		
All ages	L	-3.00

Table 4-3 indicates the ground condition unit and relative intensity that correspond to the geologic units of the geologic map. Figure 4-14 shows the conterminous United States mapped in terms of these seismic units.

Scenario Earthquakes. Based on the earthquakes discussed above, representative of all major regions of the conterminous United States, eight scenario events were selected for this investigation. The eight events are indicated in Table 4-4. With the exception of the Cape Ann, Charleston, and Hayward events, all magnitudes are reflective of the representative earthquake for the region (as specified in Table 4-2). The scenario events for Cape Ann, Charleston, and Hayward have magnitudes one-half unit higher than the representative event. These magnitudes are interpreted as maximum credible for these locations.

The choice of a scenario event on the Hayward fault for the San Francisco Bay Area, rather than the 1906 San Francisco event, is based on the perceived high likelihood of a magnitude 7.0 event (USGS, 1990) as well as the potential for major damage and lifeline disruption, should such an event occur (CDMG, 1987). Since most lifelines approach San Francisco Bay from the east, more of them cross the Hayward Fault than cross the San Andreas Fault. So the

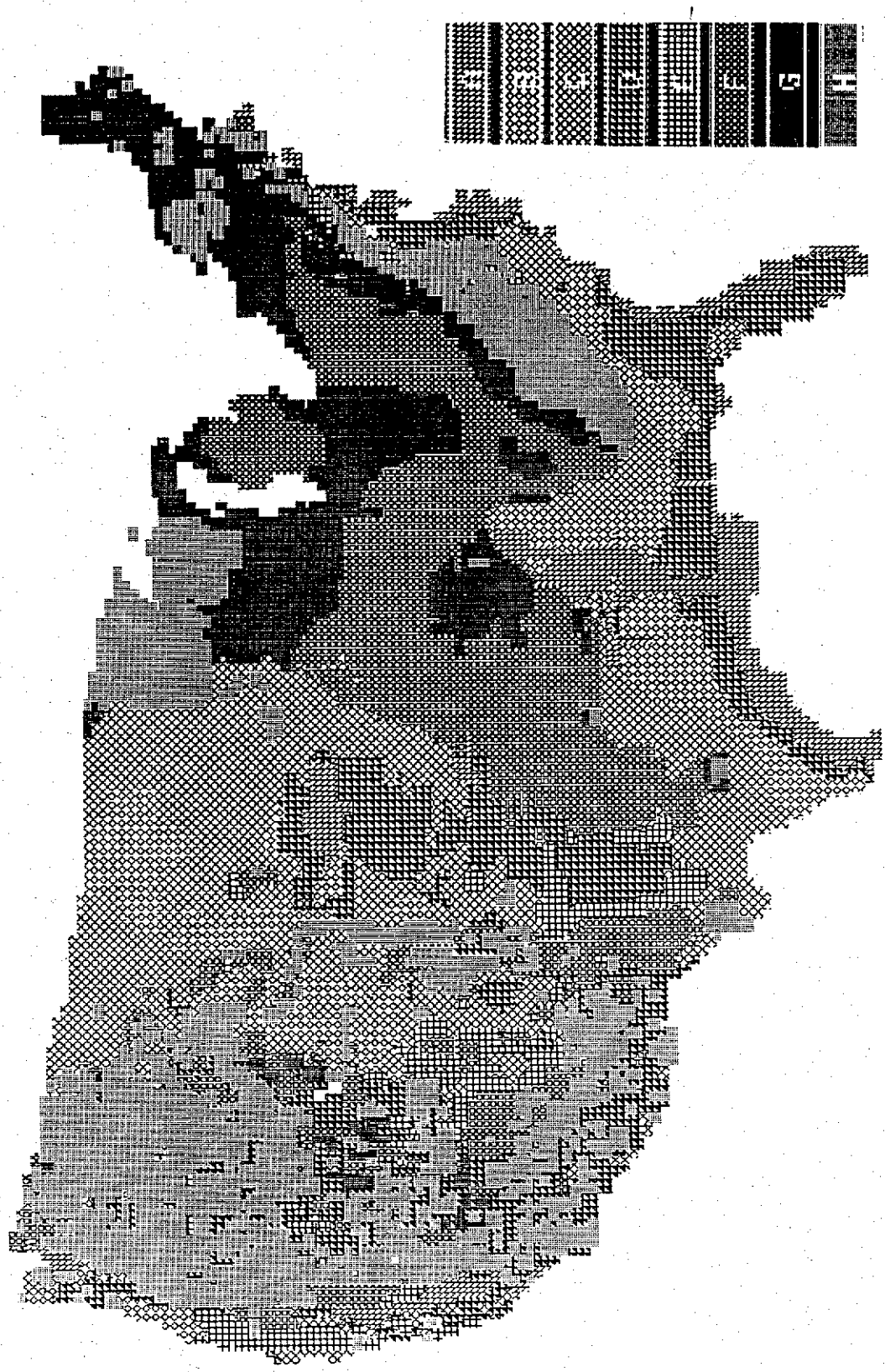

Figure 4-14 *Map of conterminous United States showing ground condition units from Evernden et al. (1981). See Table 4-3 for explanation of units.*

Table 4-4 Scenario Earthquakes

Region	*Event*	*Magnitude*
Northeastern	Cape Ann	7
Southeastern	Charleston	7.5
Central	New Madrid	7 and 8
Western Mountain	Wasatch Front	7.5
Northwestern	Puget Sound	7.5
Southern California	Fort Tejon	8
Northern California	Hayward	7.5

Hayward event would appear to represent as disruptive an event, and potentially more so, than the 1906 event, which is presently perceived to be of low likelihood in the near future.

Intensity Distributions. The Evernden model was employed to generate expected seismic intensity distribution in the conterminous United States for the eight scenario events. These intensity distributions are presented in Figures 4-15 through 4-22.

The intensity patterns for these events are seen to be basically circular, centered at the earthquake's epicenter. Deviations from the circular shape are due to local geologic conditions. Comparison of estimated intensities with historic event isoseismals indicates general agreement, though historical events are in some cases smaller than the scenario event.

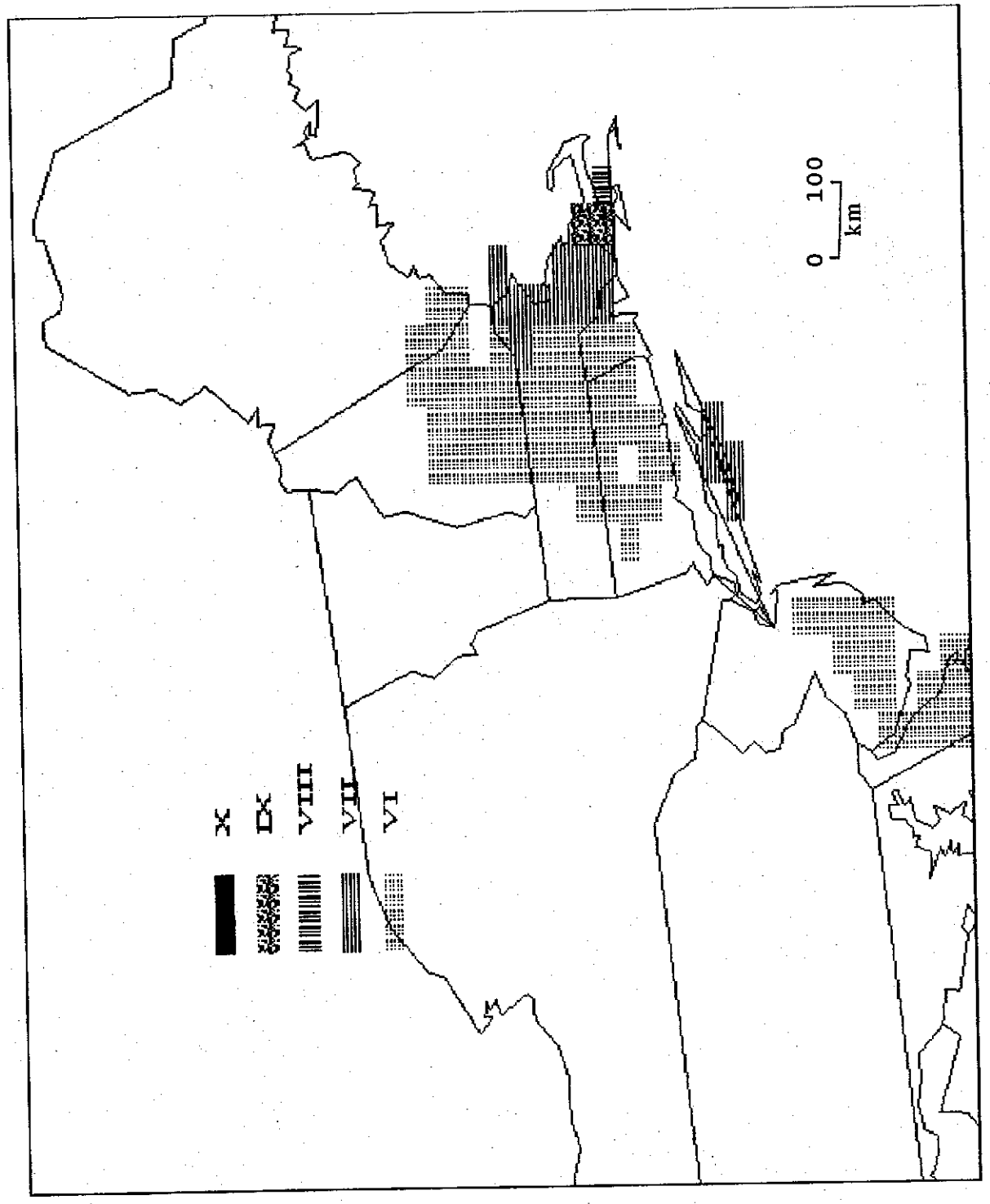

Figure 4-15 Predicted intensity map for Cape Ann (Magnitude 7).

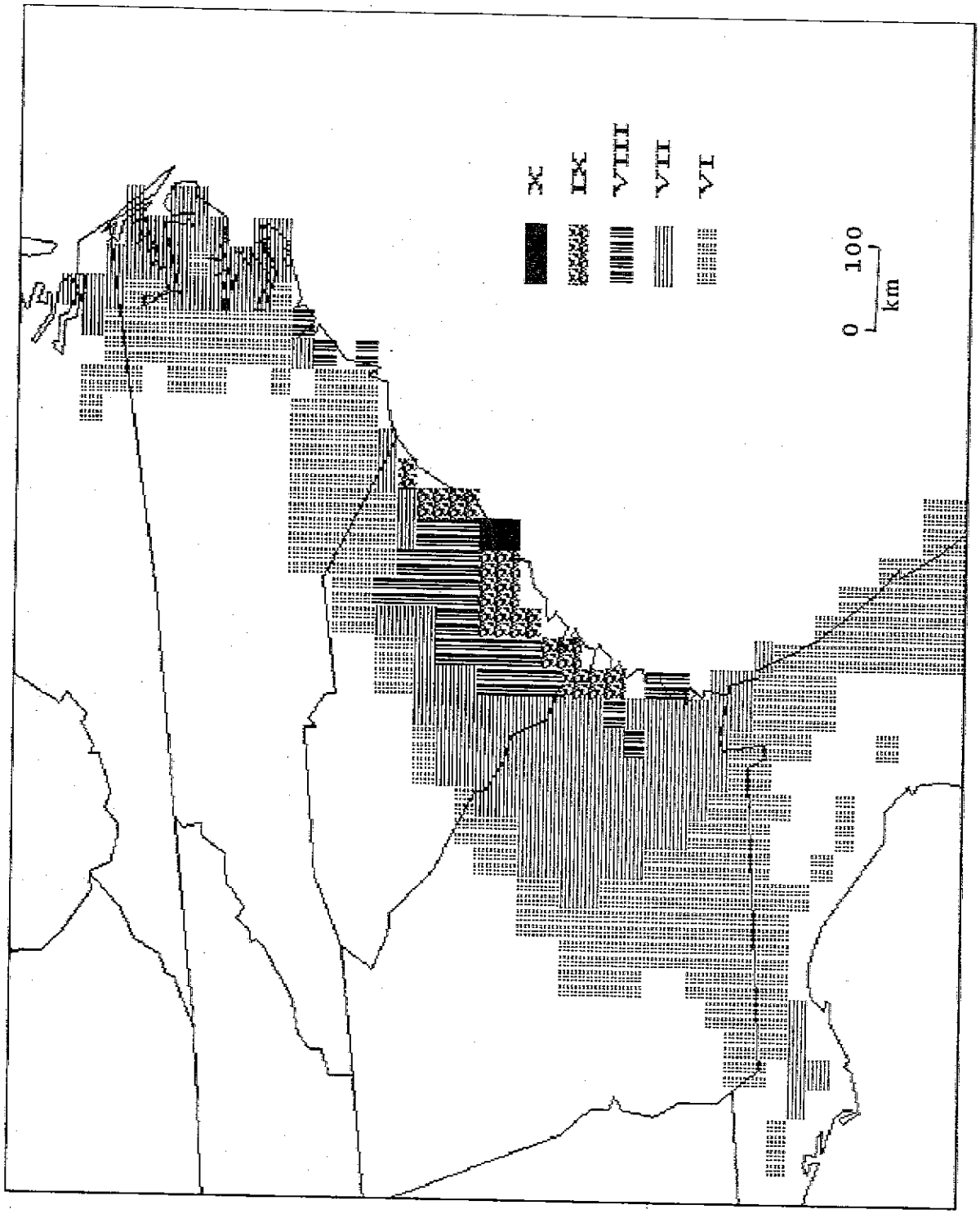

Figure 4-16 Predicted intensity map for Charleston (Magnitude 7.5).

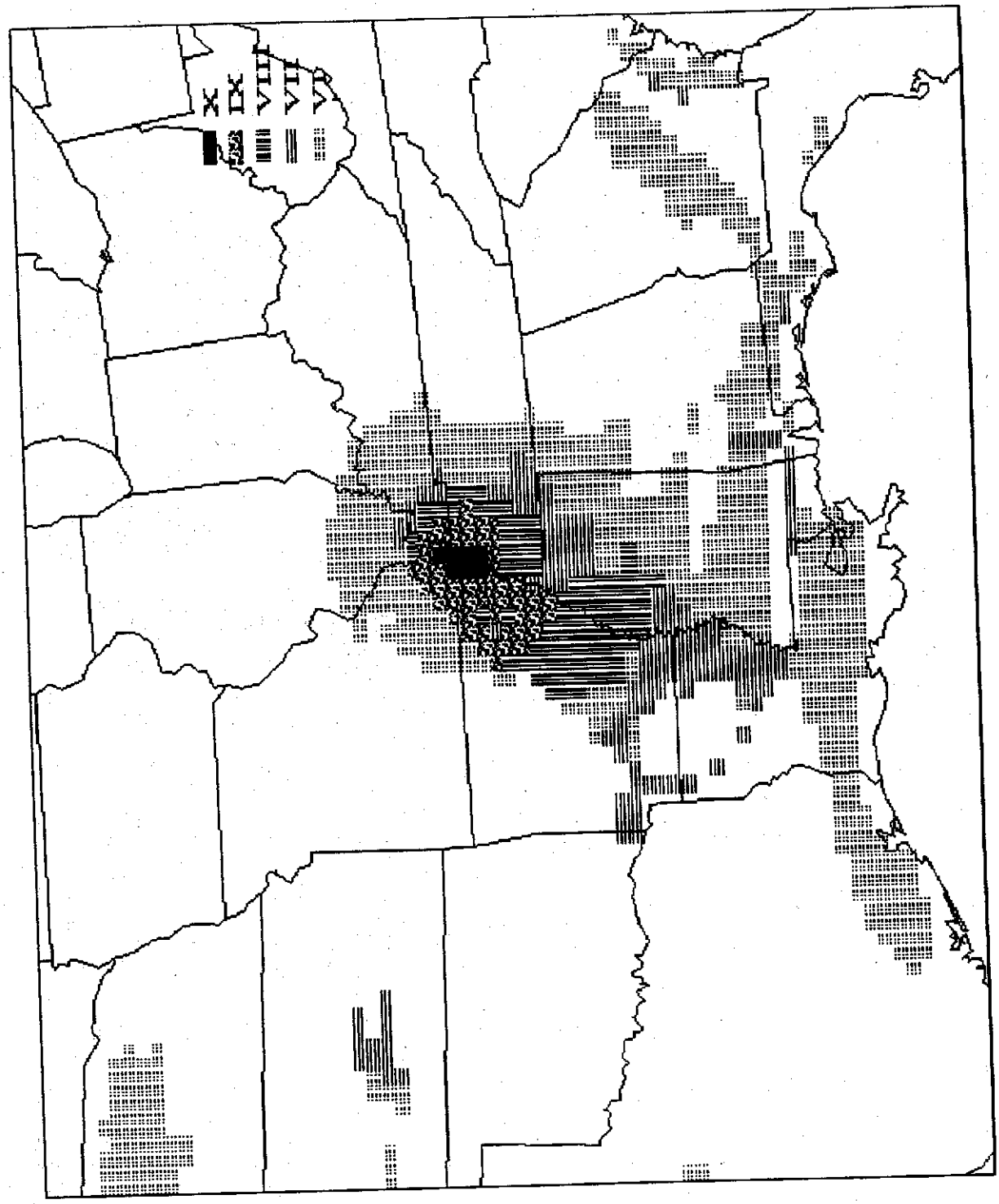

Figure 4-17 *Predicted intensity map for New Madrid (Magnitude 8).*

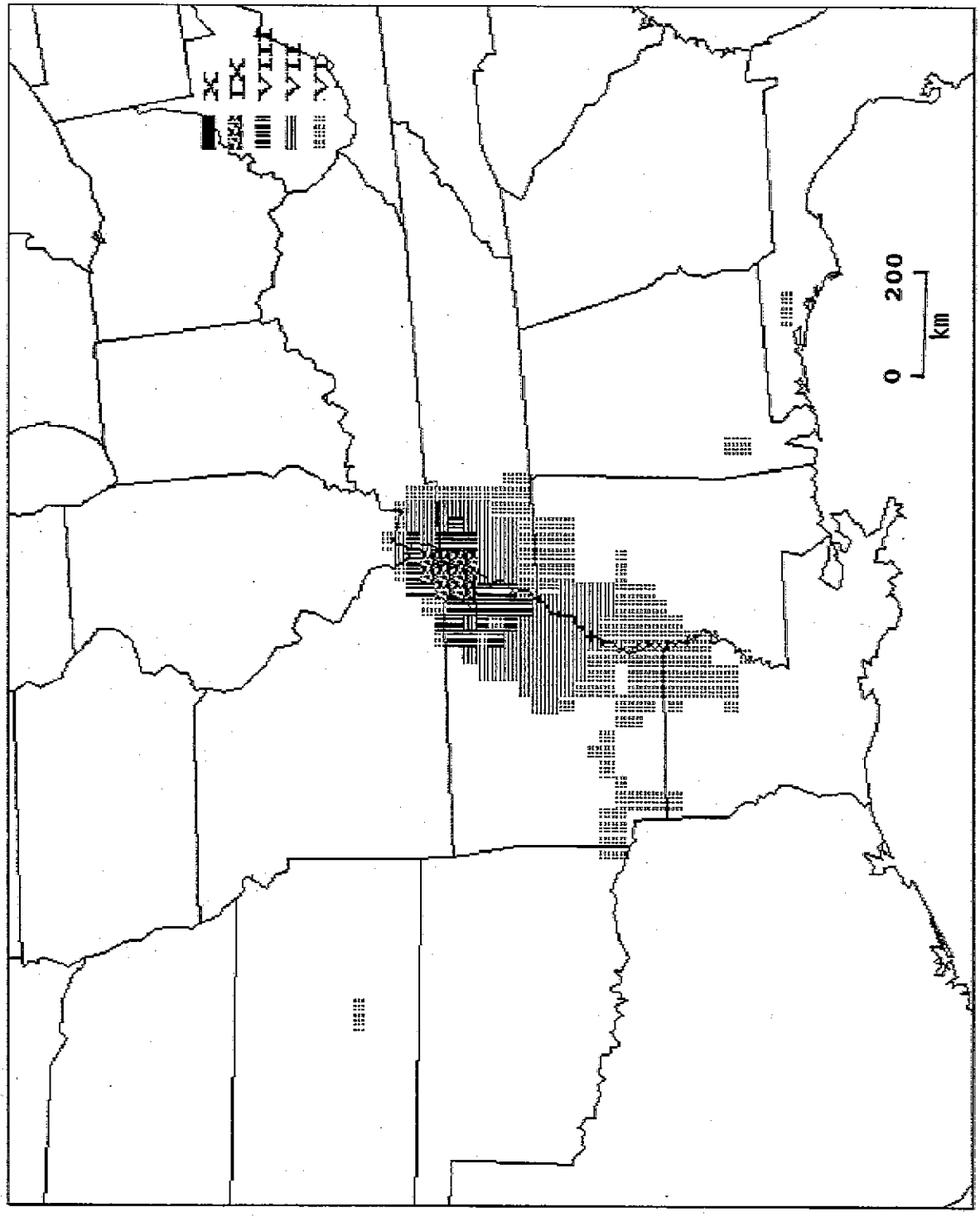

Figure 4-18 Predicted intensity map for New Madrid (Magnitude 7).

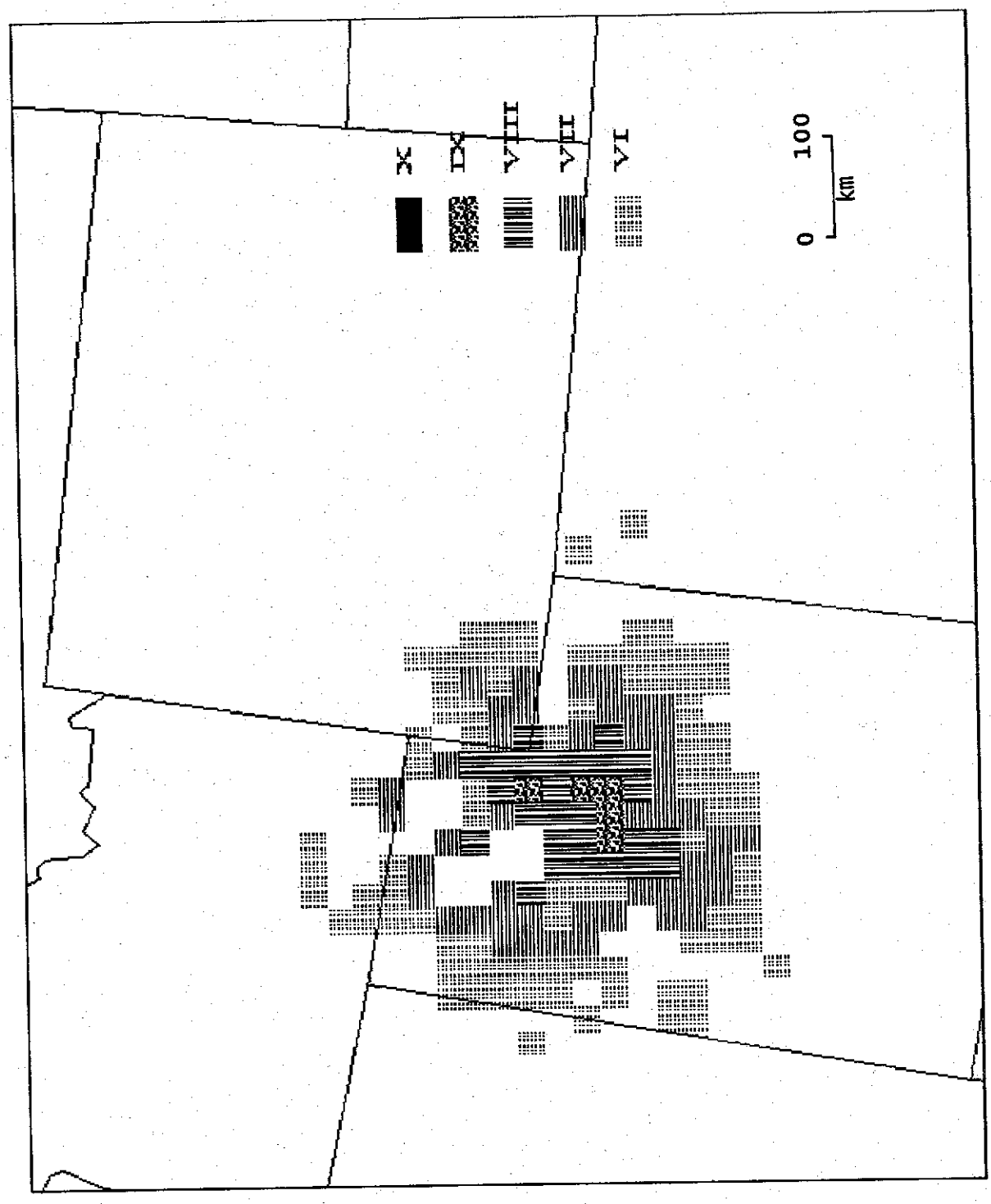

Figure 4-19 *Predicted intensity map for Wasatch Front (Magnitude 7.5).*

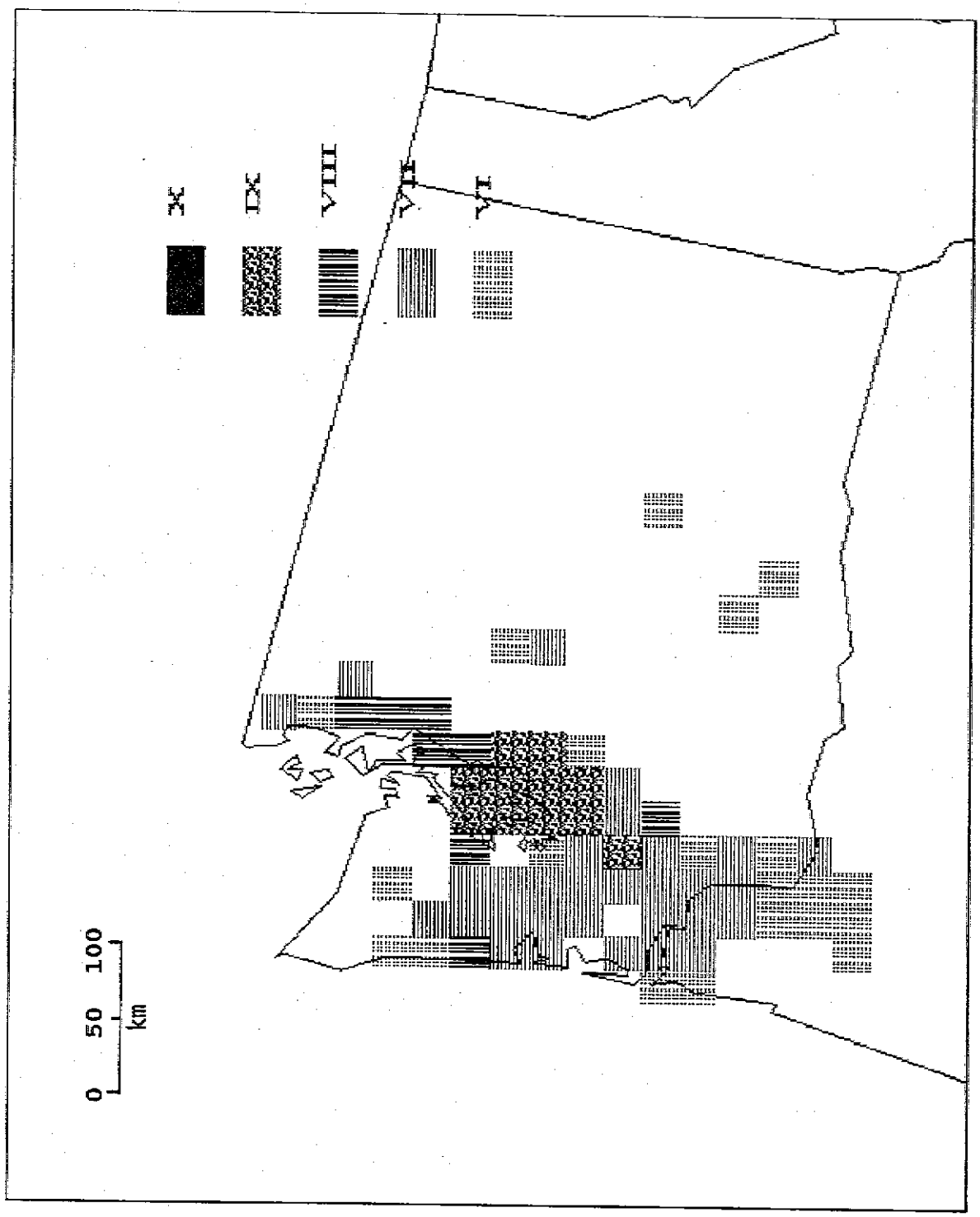

Figure 4-20 Predicted intensity map for Puget Sound (Magnitude 7.5).

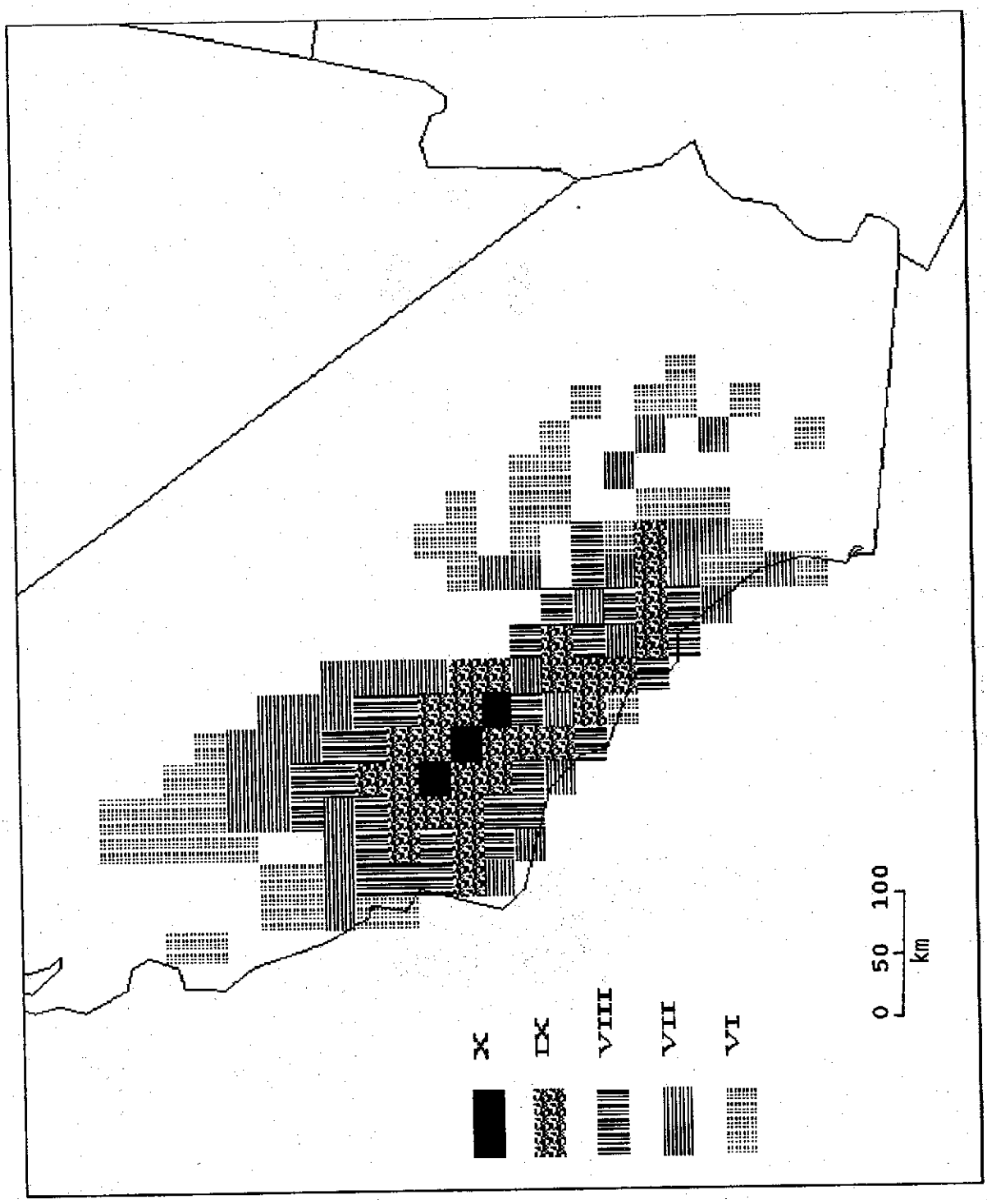

Figure 4-21 Predicted intensity map for Fort Tejon (Magnitude 8).

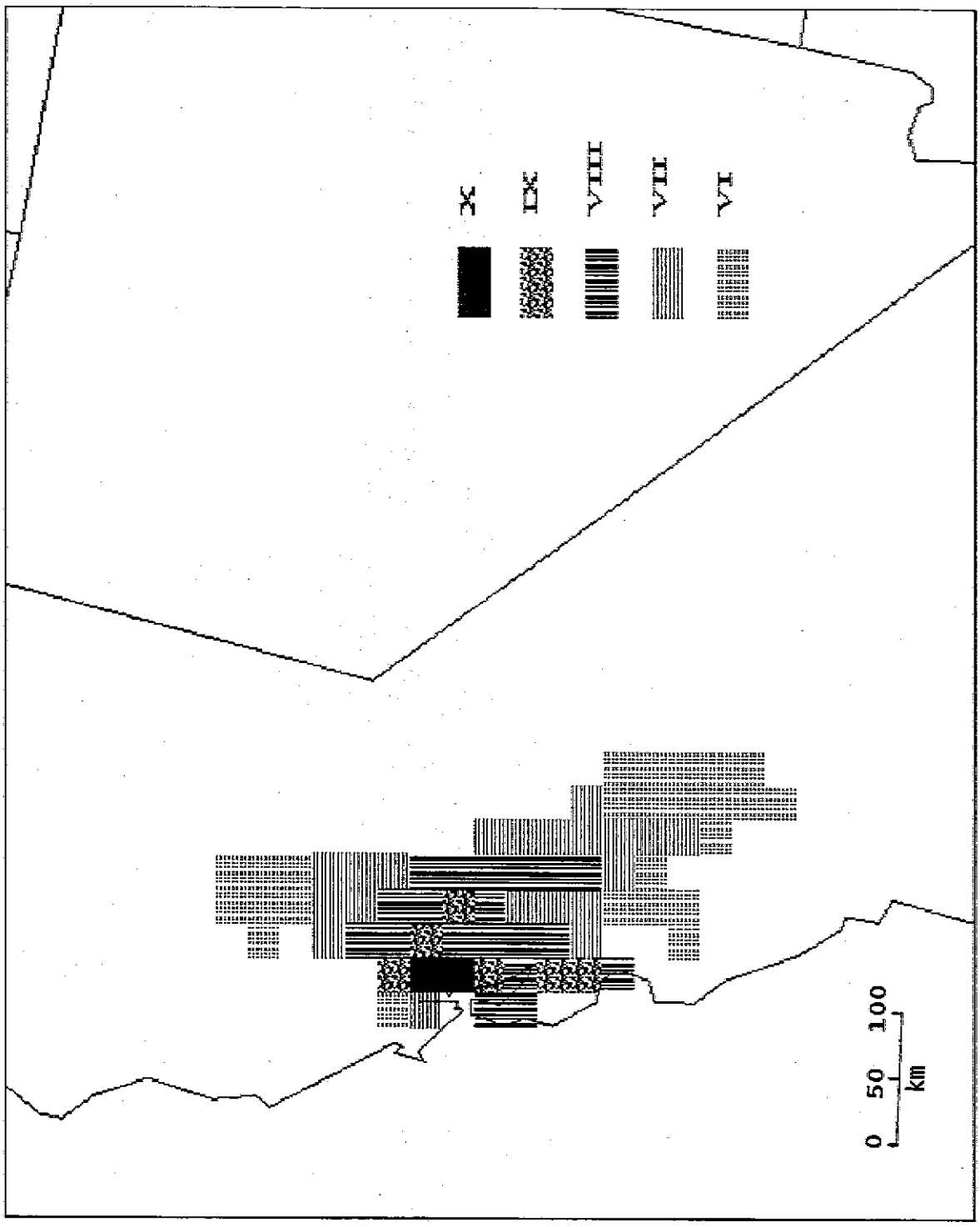

Figure 4-22 Predicted intensity map for Hayward Fault (Magnitude 7.5).